Monthly Notices
of the
ROYAL ASTRONOMICAL SOCIETY

MNRAS **499,** 5121–5135 (2020)
Advance Access publication 2020 October 15

doi:10.1093/mnras/staa3173

The dependence of Type Ia Supernovae SALT2 light-curve parameters on host galaxy morphology

M. V. Pruzhinskaya,[1]★ A. K. Novinskaya,[1,2] N. Pauna[3] and P. Rosnet[3]

[1]*Lomonosov Moscow State University, Sternberg Astronomical Institute, Universitetsky pr. 13, Moscow 119234, Russia*
[2]*Lomonosov Moscow State University, Faculty of Physics, Leninskie Gory, 1-2, Moscow 119991, Russia*
[3]*Université Clermont Auvergne, CNRS/IN2P3, LPC, F-63000 Clermont-Ferrand, France*

Accepted 2020 October 9. Received 2020 October 6; in original form 2020 June 19

ABSTRACT

Type Ia Supernovae (SNe Ia) are widely used to measure distances in the Universe. Despite the recent progress achieved in SN Ia standardization, the Hubble diagram still shows some remaining intrinsic dispersion. The remaining scatter in supernova luminosity could be due to the environmental effects that are accounted for as mass step correction in the current cosmological analyses. In this work, we compare the local and global colour ($U - V$), the local star formation rate, and the host stellar mass to the host galaxy morphology. The observed trends suggest that the host galaxy morphology is a relevant parameter to characterize the SN Ia environment. Therefore, we study the influence of host galaxy morphology on light-curve parameters of SNe Ia from the PANTHEON cosmological supernova sample. We determine the Hubble morphological type of host galaxies for a subsample of 330 SNe Ia. We confirm that the SALT2 stretch parameter x_1 depends on the host morphology with the p-value $\sim 10^{-14}$. The supernovae with lower stretch value are hosted mainly by elliptical and lenticular galaxies. No correlation for the SALT2 colour parameter c is found. We also examine Hubble diagram residuals for supernovae hosted by 'early-type' and 'late-type' morphological groups of galaxies. The analysis reveals that the mean distance modulus residual in early-type galaxies is smaller than the one in late-type galaxies, which means that early-type galaxies contain brighter supernovae after stretch and colour corrections. However, we do not observe any difference in the residual dispersion for these two morphological groups. The obtained results are in the line with other analyses showing environmental dependence of SN Ia light-curve parameters and luminosity. We confirm the importance of including a host galaxy parameter into the standardization procedure of SNe Ia for further cosmological studies.

Key words: supernovae: general – galaxies: general – distance scale.

1 INTRODUCTION

Type Ia Supernovae (SNe Ia) stand out among the other types of supernovae in that they have smaller luminosity dispersion at maximum light and show higher optical luminosities. These two properties allowed us to use them as cosmological distance indicators that led to the discovery of the accelerating expansion of the Universe (Riess et al. 1998; Perlmutter et al. 1999). The most recent analysis of SNe Ia indicates that considering the flat ΛCDM cosmology, the Universe is accelerating with $\Omega_\Lambda = 0.702 \pm 0.022$ (Scolnic et al. 2018; Abbott et al. 2019).

When the first supernova light curves (LCs) had been collected and analysed, Walter Baade noticed that SNe are more uniform than novae, which makes them suitable as extragalactic distance indicators (Baade 1938). That time, Rudolph Minkowski has not yet divided SNe into two main types, Type I and Type II (Minkowski 1941). However, the idea that had been first expressed by Baade was confirmed later for Type Ia supernovae. It is how the 'standard candle' hypothesis appeared.

Now we know that the similarity of SN Ia light curves and luminosities is explained by the similarity of the physical processes that lead to the outburst phenomenon that arises from a thermonuclear explosion of C–O white dwarf (Hoyle & Fowler 1960). In fact, when the detailed observations of a large number of supernovae had been accomplished, it became clear that the absolute magnitude at maximum can vary within ∼1 mag and even more for some SN Ia subclasses (e.g. Ashall et al. 2016). The reasons of luminosity dispersion could be different. First, we are still uncertain about the nature of the progenitor systems of SNe Ia. It can be the 'single-degenerate' (SD) scenario where the burst is a result of the matter accretion on a white dwarf from a companion star (Whelan & Iben 1973) or the 'double-degenerate' (DD) scenario that is the merger of two white dwarfs (Iben & Tutukov 1984; Webbink 1984). To explain the peculiar Type Ia Supernovae (91bg-like, Iax, 91T-like, 03fg-like) there exist some alternative scenarios, like sub-Chandrasekhar, that is usually associated with weak explosions, or super-Chandrasekhar scenario for more luminous events (Fink et al. 2018; Polin, Nugent & Kasen 2019; Hsiao et al. 2020). These scenarios have internal freedom that results in significant variations in observed light curves of SNe Ia: like point of deflagration-to-detonation transition (for SD scenario) or difference in total mass of merging white dwarfs (for DD scenario).

Another important factor which could violate the 'standard candle' hypothesis is dust. Dust around the supernovae, as well as in the host galaxy, surely affects light-curve behaviour. The distribution and the

★ E-mail: pruzhinskaya@gmail.com

properties of dust in host galaxies of supernovae could be different from that in the Milky Way. In the recent paper of Brout & Scolnic (2020), it is also suggested that the dominant component of observed SN Ia intrinsic scatter is from R_V variation of dust around a supernova.

In addition, the initial chemical composition of the progenitor stars also complicates the picture. Timmes, Brown & Truran (2003) suggested that low-metallicity progenitors produce more ^{56}Ni and therefore more luminous SNe Ia. Moreover, a lower metallicity involves an increase of the Chandrasekhar limit. Indeed, according to Bogomazov & Tutukov (2011) the average energy of SNe Ia should increase from the redshift $z > 2$ and increase significantly from the redshift $z > 8$, since at the early stages of the Universe evolution more massive white dwarfs merged on average than now. However, so distant Type Ia Supernovae are not yet discovered.

Moreover, SNe Ia explode in all types of galaxies that have an environment with different properties. In elliptical galaxies or in halo of spiral galaxies only old, i.e. metal-poor, stars with an age comparable to that of the Universe are located. On the contrary, in the star formation regions of spiral galaxies there are young metal-rich stars. These factors (the age, the chemical composition of the region around a supernova, the presence of dust) could be considered as the environmental effects.

Fortunately, it was established that supernovae are partly 'standardizable candles' (see Section 2.1), that allowed us to improve a lot of the accuracy of distance measurements and to reduce the intrinsic dispersion of SNe Ia on the Hubble diagram to 0.11 mag (Betoule et al. 2014; Scolnic et al. 2018). A part of the remaining scatter in supernova luminosity could be due to the environmental effects that are not accounted by the current standardization methods. Therefore, the SN Ia standardization procedure is one of the main sources of systematic uncertainties in the cosmological analyses.

In this paper, we study how the host galaxy morphology affects the light-curve parameters of Type Ia SNe and therefore, their luminosity. The analysis is based on the most up-to-date cosmological sample of SNe Ia, PANTHEON (Scolnic et al. 2018). The paper is organized as follows. In Section 2, we describe the current supernova standardization procedure and compare the different approaches to characterize the supernova environment. In Section 3, we describe the PANTHEON supernova sample and host morphological classification; we also show there how the host morphology affects the SN Ia light-curve parameters and the Hubble diagram residuals. In Section 4, we compare our results with the ones for other environmental parameters. Finally, we conclude this study in Section 5.

2 ENVIRONMENTAL EFFECTS

2.1 Supernova standardization

The use of Type Ia Supernovae to measure the cosmological parameters of the Universe would never be possible without the discovery of the relation between the peak luminosity of SNe Ia and their light-curve decline rate after the maximum light. The relation was independently discovered by B. W. Rust and Yu. P. Pskovskii in the 1970s (Rust 1974; Pskovskii 1977, 1984). It was also confirmed by M. Phillips on a new level of accuracy using the better supernova sample (Phillips 1993). The relation shows that the light curves of more luminous supernovae have slower decline rate after the maximum light. Later it has been found that SN Ia absolute magnitude depends on the supernova colour as well (Hamuy et al. 1996a; Tripp 1998).

Nowadays more sophisticated parameters describing supernova observational properties are used to standardize SNe Ia. Among the most recent models of SN Ia parametrization are SALT2 (Guy et al. 2007), SNEMO (Saunders et al. 2018), and SUGAR (Léget et al. 2020).

To characterize the supernova LCs, we use SALT2 x_1 (stretch) and c (colour) parameters. The x_1 parameter describes the time-stretching of the light curve. The c parameter is the colour offset with respect to the average at the date of maximum luminosity in B-band, i.e. $c = (B - V)_{\max} - \langle B - V \rangle$. We adopt the classical standardization equation of the distance modulus:

$$\mu = m_B^* - M_B + \alpha x_1 - \beta c, \quad (1)$$

where m_B^* – value of the B-band apparent magnitude at maximum light, M_B is a standardized absolute magnitude of the SNe Ia in B-band for $x_1 = c = 0$; α and β describe, consequently, the stretch and colour law for the whole SN Ia population.

2.2 Local versus global parameters

The environment of SNe Ia can be characterized by different parameters that we roughly divide into global and local. The global parameters are related to the whole host galaxy of supernova. It can be the host galaxy morphology, the metallicity, the stellar mass, the global colour, or the star formation rate (SFR). The local parameters are the same physical quantities but in turn characterizing the environment in a few kiloparsecs around a supernova, i.e. the local colour, the local SFR, the local specific SFR, etc. It is obvious that the local parameters provide more accurate description of the SN environment. However, the current state of the data processing and the resolution of the largest telescopes do not allow us to measure the local parameters at high redshifts with a good accuracy or it becomes a very time-consuming process. That is why a study of influence of the local parameters on the SNe Ia properties is based mainly on the low-redshift supernova samples. For example, the most recent analysis of the local specific SFR in 1 kpc region around a supernova is done for 141 objects of the Nearby Supernova Factory (Aldering et al. 2002) with redshift $0.02 < z < 0.08$ (Rigault et al. 2018). From that point it is more expedient to use the global parameters, for example, host galaxy morphology. At the moment, it is possible to determine the morphology of the most distant Hubble galaxies with $z > 1$ (Meyers et al. 2012), which makes the study of host morphology impact possible even for cosmological supernovae.

Moreover, the number of discovered supernovae increases dramatically. In the epoch of the Legacy Survey of Space and Time (LSST; LSST Science Collaboration 2009) millions of SNe will be discovered every year. In this sense, the accurate measurements of the local environmental parameters for each supernova become very expensive since it requires time on the largest telescopes. The global parameters on the contrary are easier to obtain by processing the images of wide-field photometric surveys with use of traditional astronomical methods as well as machine learning techniques (e.g. Domínguez Sánchez et al. 2018).

It is worth to stress that the local and global parameters correlate to each other. For example, the local $(U - V)$ rest-frame colour in a region of 3 kpc around a supernova correlates with the stellar mass of the host so that the most massive galaxies are those for which the nearby supernova environment is red (see fig. 10 of Roman et al. 2018). Here, we consider how the host morphology correlates with the local and other global parameters of environment. To do that we determine the supernova host morphology of 89 supernovae from Rigault et al. (2015) and 103 supernovae

from Roman et al. (2018) using SIMBAD[1] (Wenger et al. 2000), HyperLEDA[2] (Makarov et al. 2014), and NED[3] (Helou & Madore 1988; Mazzarella & NED Team 2007) astronomical data bases. To perform the comparison we use the local and global $(U-V)$ colour, the host galaxy stellar mass (Roman et al. 2018), and the local star formation rate (Rigault et al. 2015). The results are given in Fig. 1. From the top subplot showing the stellar mass of galaxy as a function of its morphology, we can see that most of the galaxies have a mass exceeding $10^{10}\,M_{\odot}$, except for irregular galaxies which are in general smaller. Beyond this observational fact related to the analysed sample, we observe the correlation between the host morphology and all considered parameters.

To quantify the ability of host galaxy morphology to account for different mass, global or local colour, or star formation rate, we perform the Welch's t-test, or unequal variances t-test (Welch 1947; Ruxton 2006). Generally speaking, this is a two-sided test for the null hypothesis that two normally distributed populations have equal means. Rather than the standard Student's t-test, Welch's t-test is more reliable when the two samples have unequal variances and/or unequal sample sizes. To perform the test we use the SCIPY.STAT PYTHON package[4] (Virtanen et al. 2020). In this version of t-test, for two independent populations n_1 versus n_2 of means μ_1 versus μ_2 and standard deviations s_1 versus s_2, the t variable supposed to follow the Student's probability law is built

$$t = \frac{\mu_1 - \mu_2}{\sqrt{\frac{s_1^2}{n_1} + \frac{s_2^2}{n_2}}}, \tag{2}$$

with a degree of freedom approximated to

$$\nu = \frac{\left(\frac{s_1^2}{n_1} + \frac{s_2^2}{n_2}\right)^2}{\frac{s_1^4}{(n_1-1)n_1^2} + \frac{s_2^4}{(n_2-1)n_2^2}}. \tag{3}$$

Once t and ν are calculated, the probability or p-value to obtain the null hypothesis is computed following the Student's t-distribution. The smaller p-value corresponds to higher separation of the two populations with respect to the variable under study or, in other words, the ability of morphology groups to account for different astrophysical properties of two populations.

The results of the t-test for the local and global parameters are reported in Table 1. We split the data into two groups according to their morphological type. We also consider three different groupings based on the dependence observed in Fig. 1. As can be seen from the Table 1, the p-value varies from about 10^{-2} down to 10^{-12}. This quantitative test shows that depending on the considered parameter the optimal splitting into two morphological groups is not the same. The SFR parameter is more powerful to separate E–S0 group from S0/a–Ir, while the stellar mass and global and local $(U-V)$ colours are better to divide the galaxies into E–Sab and Sb–Ir groups. Therefore, this analysis suggests that the morphological type of a galaxy is a powerful parameter to separate the galaxy properties w.r.t. the colour and the star formation rate. In conclusion, the grouping from E to S0/a morphology versus Sa to Ir is a good compromise to correlate both colours (local and global) and SFR with the two populations referred to below as 'early-type' (E–S0/a) and 'late-type' (Sa–Ir) morphological groups.

[1] http://simbad.u-strasbg.fr/simbad/
[2] http://leda.univ-lyon1.fr/
[3] https://ned.ipac.caltech.edu/
[4] https://docs.scipy.org/doc/scipy/reference/generated/scipy.stats.ttest_ind.html

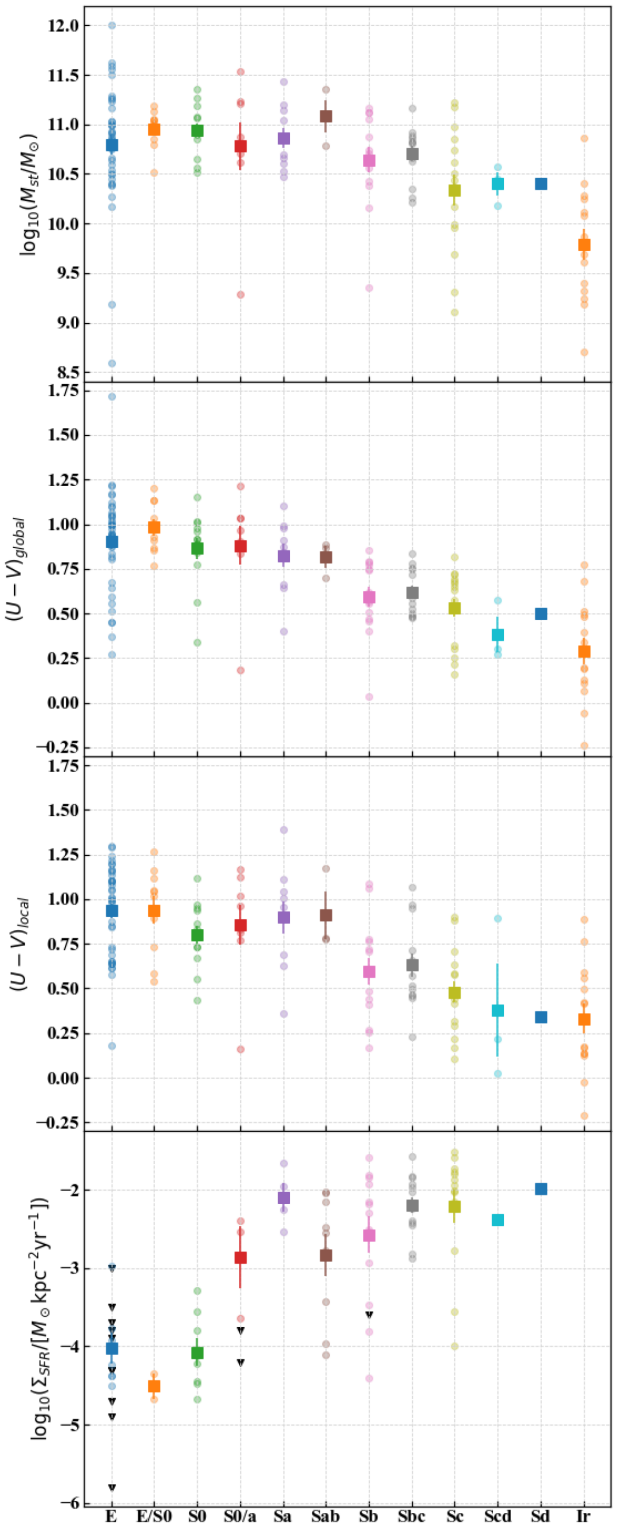

Figure 1. Stellar mass, global $(U-V)$ colour, local $(U-V)$ colour in 3 kpc region around SN Ia, and local star formation rate in 1 kpc region around SN Ia versus morphological type of the supernova hosts for the SN subsamples from Roman et al. 2018 (three upper subplots) and from Rigault et al. 2015 (lower subplot). Mean values of the data points and associated standard deviations in each morphological bin are marked with squares with error bars. The upper limits on the local SFR are marked with triangles.

Table 1. *p*-values of the Welch's *t*-test for the different morphological groupings corresponding to Fig. 1 with respect to each global and local parameter.

Morph. group	$\log_{10}(M_{st}/M_{\odot})$	$(U-V)_{\rm global}$	$(U-V)_{\rm local}$	$\log_{10}(\Sigma_{\rm SFR}/[M_{\odot}{\rm kpc}^{-2}{\rm yr}^{-1}])$
E–S0 | S0/a–Ir	2.6×10^{-2}	6.2×10^{-9}	1.2×10^{-6}	1.7×10^{-7}
E–S0/a | Sa–Ir	1.7×10^{-2}	3.3×10^{-10}	3.4×10^{-7}	7.0×10^{-7}
E–Sab | Sb–Ir	6.6×10^{-4}	6.2×10^{-13}	2.4×10^{-10}	1.7×10^{-4}

Taking into account all of the above, in this work we use host galaxy morphology to describe the supernova environment and we study its impact on the PANTHEON (Scolnic et al. 2018) cosmological sample of supernovae.

3 DEPENDENCE OF SN IA PROPERTIES ON HOST GALAXY MORPHOLOGY

In this section, we examine the dependencies of the supernova light-curve parameters and luminosity on host morphology using SNe Ia from the PANTHEON sample.

3.1 PANTHEON supernova sample

Cosmological supernova sample PANTHEON consists of 1048[5] spectroscopically confirmed SNe Ia with redshifts up to $z \simeq 2.3$ (Scolnic et al. 2018). PANTHEON sample represents a compilation from several supernova surveys: 172 objects were taken from the nearby supernova surveys ($0.01 < z < 0.1$), 334 objects from the Sloan Digital Sky Survey (SDSS; Frieman et al. 2008; Kessler et al. 2009), 236 from the SuperNova Legacy Survey (SNLS; Guy et al. 2010; Conley et al. 2011), 279 objects from the Pan-STARRS survey (PS1; Rest et al. 2014; Scolnic et al. 2014), and 26 SNe were discovered by the *Hubble Space Telescope* (*HST*; Riess et al. 2004, 2007; Suzuki et al. 2012; Graur et al. 2014; Rodney et al. 2014; Riess et al. 2018). PANTHEON is the largest spectroscopic cosmological SN sample to date. The main advantages of PANTHEON compared to the previous compilations are: an intercalibration between different surveys and a thorough investigation of systematic uncertainties.

3.2 Morphological classification of host galaxies

To analyse how the morphological type of host galaxy affects the supernova luminosity and standardization parameters, we first determine the host morphology according to the Hubble morphological classification (Hubble 1926, 1936; de Vaucouleurs 1959). To do that, we use SIMBAD, HyperLEDA, and NED astronomical data bases as well as individual publications.

Unfortunately, it is not possible to find the detailed morphological classification for all supernova hosts, especially at high redshifts. For some supernovae, we could only define either they belong to star-forming (SF) or passive (Pa) galaxies. For high-z SNe Ia we use a classification from Meyers et al. (2012) and Rodney et al. (2014). Meyers et al. (2012) only distinguish passively evolving early-type galaxies from star-forming late-type galaxies. In Rodney et al. (2014) SN hosts are classified visually into three main morphological categories (spheroid, disc, irregular) and two intermediate categories (spheroid+disc and disc+irregular). These morphological classes roughly correspond to broad bins over the Hubble sequence: spheroid (E/S0), spheroid+disc (S0/Sa), disc (Sb/Sbc/Sc), disc+irregular (Sc/Scd), irregular (Scd/Ir). It should be noticed that there are only a few high-z *HST* supernovae and all of them, as well as their hosts, were subjected to the comprehensive astrophysical analysis in previous works. However, there are no such detailed studies for the host galaxies of SNLS supernovae. It explains the absence of morphological classification of supernova hosts at redshift $z \sim 0.4$–1.

[5]The exact number is 1047, since one supernova was counted twice under the different names, SN2005hj and SN6558.

Table 2. Contribution of the different surveys to the PANTHEON cosmological sample and the subsample of 330 SNe Ia used in this work.

Survey	PANTHEON	This work
low-z	172	166
PS1	279	12
SDSS	334	133
SNLS	236	1
HST	26	18
Total	1047	330

Based on these sources, we found the host morphology of 330 SNe Ia from the PANTHEON sample. The result of this classification is given in Table A1 (Appendix A). Columns 1 and 2 contain the supernova name and PANTHEON ID, where 0 corresponds to low-z, 1 – PS1, 2 – SDSS, 3 – SNLS, and 4 – *HST* supernova sample. Column 3 contains the supernova redshift relative to the CMB frame. Host galaxy name is in column 4. The morphology extracted from SIMBAD, HyperLEDA, and NED are given in columns 5, 6, 7, respectively. When the morphological classification provided by the different data bases is controversial, we thoroughly analysed its primary source and defined a final type in column 8. In few cases, the morphological classification is drawn out from the individual publications that we cite in column 9. The contribution of the different surveys to the subsample of 330 SNe is presented in Table 2.

In Fig. 2, we show the distribution of 330 SNe with known host morphology by redshift, stretch, and colour parameters relative to the whole PANTHEON supernova sample. Bottom subplots show the ratio between the number of objects used in this work and in the whole PANTHEON sample in each $z_{\rm CMB}$, x_1, and c bin. It can be noticed that our analysis is biased w.r.t. the redshift since the galaxy morphology as any other environmental parameter is easier to determine at low redshifts. However, in terms of stretch and colour parameters our subsample is quite good representative of the PANTHEON supernova sample.

3.3 Results

The final distribution of SNe Ia by host morphological type is summarized in Table 3. As we can see from Table 3, the distribution of the SN hosts by the morphological types is uneven. Moreover, while for the nearby galaxies the detailed Hubble classification is usually available, for the distant ones it is rather simplified. Therefore, for the further analysis we combine the 'close' morphological types in two

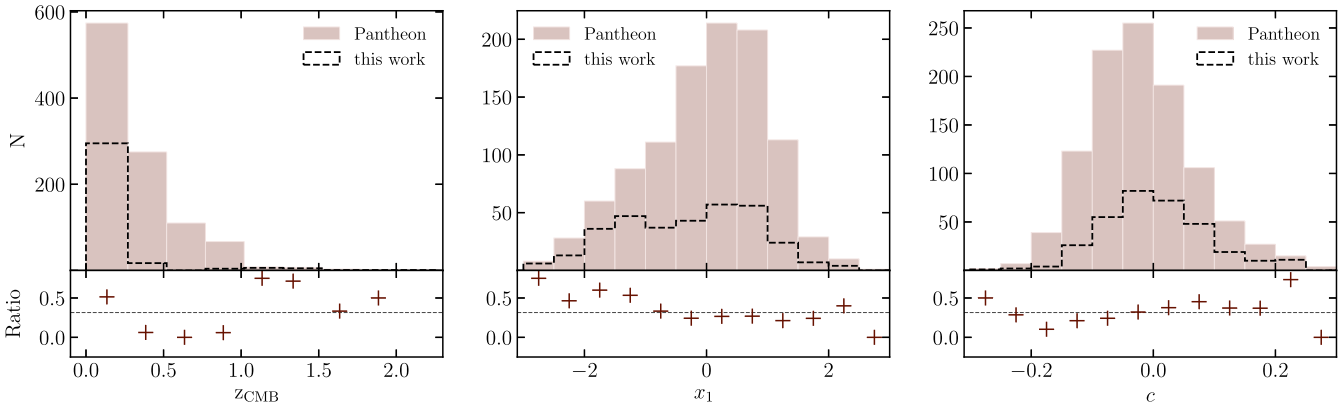

Figure 2. Distribution of SNe Ia by redshift (z_{CMB}) and LC parameters such as stretch (x_1) and colour (c) for the whole PANTHEON sample and for its subsample of 330 SNe Ia used in this work. Bottom subplots show the ratio between the number of objects in our subsample and in the PANTHEON sample for each bin (crosses) and in total (dashed horizontal line).

Table 3. Distribution of the host galaxies of the PANTHEON SN Ia subsample according to their morphological type.

Early-type (6)	
Pa (15)	
E (28)	Early-type (91)
E/S0 (18)	
S0 (12)	
S0/a (12)	
Sa (21)	
Sab (16)	
Sb (37)	
Sbc (37)	
Sc (37)	
Sb/Sbc/Sc (1)	Late-type (239)
Scd (3)	
Sd (1)	
Scd/Ir (1)	
Ir (30)	
SF (48)	
Late-type (7)	

groups: 'early-type' and 'late-type' (see Table 3). This classification in two groups is guided by the correlation observed between the host morphology and environmental parameters, as described in Section 2.2. To the former group, we assign all elliptical and lenticular galaxies as well as those classified as early-type or passive. From the environmental point of view, these galaxies are dominated by the old, low-metallicity stars due to the low star formation rate. They are also relatively free from dust. The latter group is quite broad and includes all spirals, star-forming, late-type, and irregular galaxies. These systems contain the stars from different stellar populations and of different chemical composition. However, unlike early-type galaxies, they constantly form the new stars.

3.4 x_1 and c parameters

We first examine the dependence of SN Ia light-curve shape and colour parameters on host morphology. Fig. 3 shows the SALT2 x_1 and c light-curve parameters as a function of host galaxy morphology for the PANTHEON SN Ia subsample. For the left subplots, we calculate the mean value of the corresponding LC parameter in each morphological bin. The mean values are marked with squares. The right subplots are the histograms of x_1 and c distribution for 'early-type' and 'late-type' morphological groups. As we are interested in the shape of the distribution, for clarity each histogram is normalized so that the integral under it equals one.

We observe that the stretch parameter constantly increases along the Hubble morphological sequence from elliptical to irregular galaxies. If we consider only two morphological groups, the difference in the stretch mean values is $\Delta_{\overline{x_1}} = 1.04$ with a significance $>8.5\sigma$ (Table 4). Therefore, SNe Ia with the fastest decline rate, i.e. the most dim ones, appear in the galaxies with an older stellar population (elliptical and lenticular galaxies). The same conclusion is obtained by previous studies based on the other supernova samples (Hamuy et al. 1995, 1996b, 2000; Riess et al. 1999; Sullivan et al. 2003; Henne et al. 2017; Kim, Kang & Lee 2019).

The difference in mean values for the colour parameter c is observed neither for detailed morphological classification nor for two morphological groups. This is consistent with the previous results obtained by Sullivan et al. (2010), Kim et al. (2019). Henne et al. (2017) found that SNe Ia in elliptical and lenticular galaxies have slightly bluer colour than others, and explained this by the fact that the spiral galaxies contain more dust which makes the supernovae redder. However, the found difference was not statistically significant.

To check the significance of the results we perform the Welch's t-test described in Section 2.2. The test confirmed that for SNe Ia exploded in 'early-type' and 'late-type' morphological groups the difference in $\overline{x_1}$ is significant with the p-value equal to $\sim 10^{-14}$. On the other hand, the p-value of the colour parameter is 0.45 which is not significant (see Table 4).

3.5 Hubble residuals

To investigate whether Type Ia Supernovae can be physically different in the separate groups due to environmental effect, we reproduce the Hubble diagram from the PANTHEON analysis. We consider the flat ΛCDM-model in which the Universe is filled with the matter (cold dark matter and ordinary matter) and the dark energy, i.e. $\Omega_m + \Omega_\Lambda = 1$. In this model, the theoretical distance modulus is given by

$$\mu_{\rm model} = 5 \log_{10} d_{\rm L} - 5, \tag{4}$$

$$d_{\rm L} = \frac{c}{H_0}(1+z) \int_0^z \frac{{\rm d}z'}{\sqrt{\Omega_\Lambda + \Omega_m (1+z')^3}}, \tag{5}$$

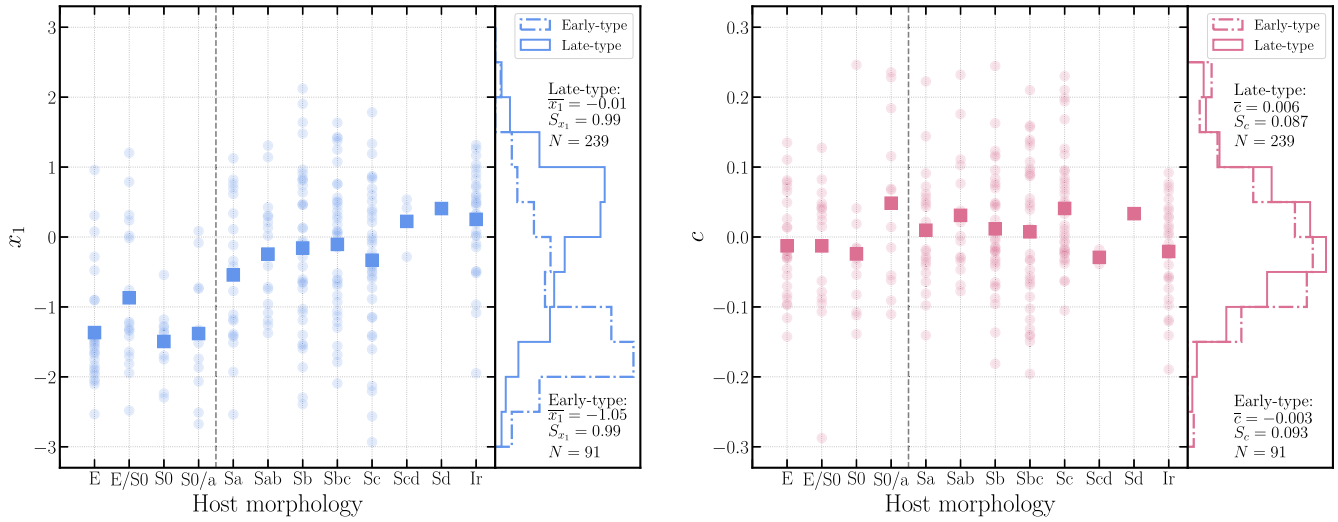

Figure 3. SALT2 x_1 and c light-curve parameters of SNe Ia depending on the host morphology. The squares denote the mean values for the corresponding parameter in each morphological bin. The right-hand subplots are the normalized histograms of x_1 and c distributions for 'early-type' and 'late-type' morphological groups.

Table 4. Mean and standard deviation of the SALT2 x_1 and c light-curve parameters and the Hubble residuals $\Delta\mu$ for 'early-type' and 'late-type' morphological groups. Last row contains the p-values of the Welch's t-test used to compare the equality of the means.

Morph. group	N	$\overline{x_1}$	S_{x_1}	$\overline{c}$	S_c	$\overline{\Delta\mu}$	$S_{\Delta\mu}$
Early-type	91	-1.05 ± 0.10	0.99	-0.003 ± 0.010	0.093	-0.092 ± 0.016	0.150
Late-type	239	-0.01 ± 0.07	0.99	0.006 ± 0.006	0.087	-0.034 ± 0.010	0.152
p-value	–	8.8×10^{-15}	–	0.45	–	2.0×10^{-3}	–

where d_L is the luminosity distance in parsecs. We assume $\Omega_\Lambda = 0.702 \pm 0.022$ (Scolnic et al. 2018). The Hubble diagram is given in Fig. 4. It can be noticed, for example, that the *HST* supernovae from the early-type hosts lie below the ones exploded in the late-type galaxies.

The observational distance modulus corresponds to the nuisance parameters given in table 6 of Scolnic et al. (2018), i.e. $\alpha = 0.154 \pm 0.006$, $\beta = 3.02 \pm 0.06$. However, it contains a distance correction based on the supernova host galaxy mass (see also Lampeitl et al. 2010; Sullivan et al. 2010; Betoule et al. 2014). The correction takes into account the correlation between host stellar mass and Hubble residuals, i.e. it is responsible for the environmental correction in the cosmological analyses. Therefore, to study the host morphology impact on the Hubble residuals we removed this correction from the observational distance modulus.

The results are given in Fig. 5 and Table 4. While from Fig. 5 it is not very clear how the residuals change along the Hubble sequence, if we divide the hosts into two morphological groups, we will see that the mean residual in the early-type galaxies is smaller than the one in the late-type galaxies. Therefore, SNe Ia in the early-type hosts are brighter after the light-curve corrections than those in the late-type. According to the Welch's t-test, this difference is significant with the p-value equal to 0.002. The same result is found in Henne et al. (2017), however Kim et al. (2019) do not observe any conclusive trend for the low-z and SDSS supernova samples.

It can be noticed that the residuals in Fig. 5 are mainly negative. To explain this, we plot the distribution of the SNe Ia subsample considered in this work by the host stellar mass (Fig. 6). For the majority of our sample $\log_{10}(M_{\rm st}/M_\odot) > 10$. Meanwhile, the fig. 14 of Scolnic et al. (2018) shows that the mean residuals for the PANTHEON SNe with $\log_{10}(M_{\rm st}/M_\odot) > 10$ are negative. Since galaxies with larger stellar mass are supposed to be more luminous, it is reasonable to suggest that it was easier to determine the morphological types of those ones than for the low-mass dim galaxies. Therefore, this is a selection effect. The fact that our subsample is biased towards the high-mass galaxies obviously has an impact. Since the low-mass galaxies tend to have more positive HD residuals, the difference in mean residuals that we observe in Fig. 5 for the early-type and the late-type galaxies is less pronounced than it could be in the absence of bias.

The host galaxy morphology could also affect the residual dispersion on the Hubble diagram. Our initial assumption is that SNe Ia should be more homogeneous in the early-type galaxies due to the similar explosion mechanism and small dust contamination (Lipunov, Panchenko & Pruzhinskaya 2011; Pruzhinskaya, Gorbovskoy & Lipunov 2011). However, we do not see any difference in the residual dispersion for early-type and late-type hosts. Moreover, some previous studies show that SNe Ia in late-type spirals (Scd-Ir) or in locally star-forming regions are more homogeneous and therefore more appropriate for cosmology (Rigault et al. 2013, 2015, 2018; Henne et al. 2017; Kim et al. 2018, 2019).

4 DISCUSSION

4.1 Comparison with the results for other environmental parameters

In Section 2.2, we show that the different parameters of environment correlate with the host morphology. Indeed, previous studies mention that the low-stretch supernovae are preferentially hosted by the galaxies with little or no ongoing star formation that is consistent

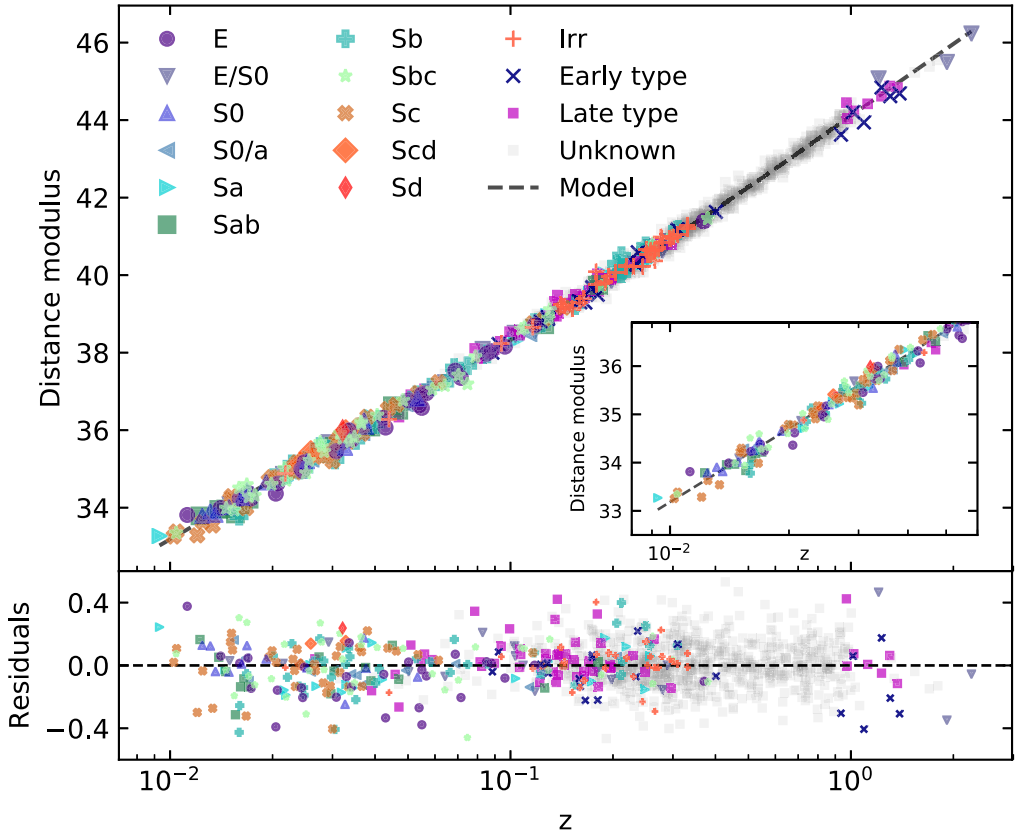

Figure 4. Hubble diagram for the PANTHEON supernovae. Different markers correspond to supernovae belonging to galaxies of different morphological types. The model corresponds to the flat ΛCDM cosmology with $\Omega_\Lambda = 0.702 \pm 0.022$ (Scolnic et al. 2018).

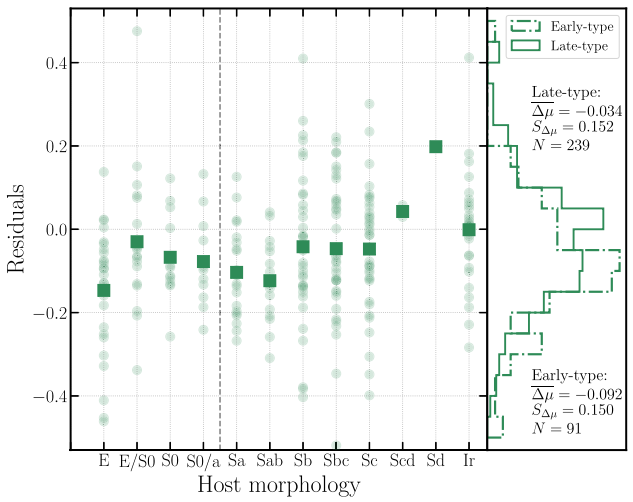

Figure 5. Hubble diagram residuals of SNe Ia depending on the host morphology. The squares denote the mean values $\Delta\mu$ in each morphological bin. The right-hand subplot is the normalized histogram of $\Delta\mu$ distribution for 'early-type' and 'late-type' morphological groups.

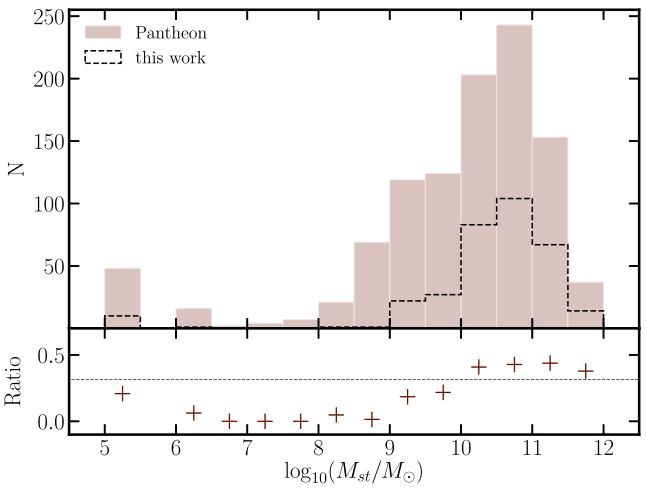

Figure 6. Distribution of SNe Ia by the host stellar mass for the whole PANTHEON sample and its subsample of 330 SNe Ia used in this work. Bottom subplot shows the ratio between the number of objects in our subsample and in the PANTHEON sample for each bin (crosses) and in total (dashed horizontal line).

with our results for the early-type galaxies (e.g. Sullivan et al. 2006; Neill et al. 2009; Sullivan et al. 2010; Smith et al. 2012; Johansson et al. 2013; Kim et al. 2019). Moreover, the analyses of Neill et al. (2009), Sullivan et al. (2010), Childress et al. (2013b), Johansson et al. (2013), Kim et al. (2019) have revealed that the observed brightness of supernovae correlates with the host stellar mass, such that the more massive hosts produce mainly fast-decline rate (low-stretch) SNe Ia. This result is consistent with ours, as illustrated by Fig. 1 showing that the early-type hosts have the highest stellar mass on average.

The relation between the colour parameter c and the different host properties is less evident. While we do not see any connection

between c and host morphology, Sullivan et al. (2010) claim that SNLS SNe Ia in low specific SFR systems do show slightly bluer colours in the mean and find no difference in SN colours in low-mass and high-mass hosts. On the contrary, Kim et al. (2019) do not observe any trend with global specific SFR but show that SNe Ia in high-mass hosts are somewhat bluer than those in low-mass hosts. Moreover, Childress et al. (2013b) notice that red SNe Ia occur in high-metallicity galaxies, the same is obtained by Moreno-Raya et al. (2016) but for the local metallicity around the regions where SNe Ia exploded. It is expected that the high-metallicity star-forming galaxies contain more dust that, therefore, should affect SN Ia colours.

Finally, previous studies show that galaxies with higher star formation rate host on average fainter supernovae after stretch and colour corrections which is consistent with our results for the late-type (star-forming) galaxies (e.g. Sullivan et al. 2010; Jones, Riess & Scolnic 2015; Kim et al. 2019).

4.2 Perspectives

The underlying motivation to use the host morphology as environmental parameter is that in contrast to the late-type galaxies, the elliptical galaxies are dominated by the old stellar population and contain the small amount of dust. However, in such approach we ignore the fact that in halo of spiral galaxies the conditions are very similar to those in elliptical ones. Thus, in the further work it seems promising to combine the morphological criteria with the information about the distance between the host centre and the supernova position. Indeed, in Hill et al. (2018) the projected galactocentric distance to the host for a subset of the SDSS SNe Ia has been investigated (see also Galbany et al. 2012). It was shown that the scatter around the Hubble diagram is less for the SNe Ia with larger galactocentric distances, i.e. they are more homogeneous. Due to the small statistics, the significance of this result is only 1.4σ, however it will be interesting to study this effect for a lager sample size and in combination with the knowledge of the host morphology.

Since there is a significant difference in the stretch parameter for 'early-type' and 'late-type' morphological groups, we also expect a difference in α nuisance parameter from equation (1). In other words, the standardization of the SN Ia luminosity variations in old environment is not the same as in young, star-forming environment (e.g. Henne et al. 2017). Therefore, instead of adding a correction term to the standardization equation (1), we could also adapt the nuisance parameter α to the SN Ia environment. For instance, two α parameters, accounting for the different morphological groups defined in this work, could be used for the Hubble diagram fit. In this way, the difference in the stretch distribution will be accounted automatically in the cosmological fit. This new approach of the SN Ia environmental correction will be tested in a coming work.

5 CONCLUSIONS

In this paper, we studied the dependencies of the different attributes of SN Ia environment, such as local and global colour ($U - V$), local SFR, and stellar mass on host galaxy morphology in order to test the reliability of the morphology as a leverage environmental parameter. We found a significant correlation of the considered parameters with the host morphology and confirmed its ability to describe the properties of the supernova host galaxies.

Then, we studied the influence of host galaxy morphology on the supernova light-curve parameters. We believe that host morphology can be a good environmental parameter for several reasons. First, it is possible that an SN explosion depends on the chemical composition of the progenitor. The elliptical galaxies contain mainly the oldest, first-generation metal-poor stars, which leads to a more homogeneous chemical composition of SN progenitors. Then, there are several progenitor scenarios that could lead to the different supernova luminosity and its LC parameters. We expect that SNe Ia in elliptical galaxies explode via the double degenerate scenario (Lipunov et al. 2011; Barkhudaryan et al. 2019). At last, the dust properties matter. Elliptical galaxies are relatively dust-free. The role of the above listed factors is difficult to evaluate in the theoretical studies, although some progress is achieved (e.g. Umeda et al. 1999; Timmes et al. 2003; Kasen, Röpke & Woosley 2009; Shen, Toonen & Graur 2017).

Using the astronomical data bases and the individual publications, we determined the Hubble morphological type of host galaxies of 330 PANTHEON SNe Ia. We confirmed that the SALT2 stretch parameter x_1 is correlated with the host galaxy type. The supernovae with a lower stretch value are hosted mainly by elliptical and lenticular galaxies. The correlation for the SALT2 colour parameter c has not been found. The analysis revealed that the mean distance modulus residual $\overline{\Delta\mu}$ in early-type galaxies is smaller than the one in late-type galaxies after standardization, which means that early-type galaxies host brighter supernovae. However, we did not see any difference in the residual dispersion for these two morphological groups. Our results for the stretch parameter and the residual values are consistent with the previous works. The conclusions concerning the colour parameter and residual dispersion are less evident since the results of the previous studies are dependent on the choice of the environmental parameter and of the supernova sample (see Section 4).

Therefore, we confirm the variation of the light-curve parameters, as well as the Hubble residuals, with morphological type of host galaxy. The including a host galaxy parameter into the SN Ia standardization and the Hubble diagram fit is expected to be important for further cosmological studies.

ACKNOWLEDGEMENTS

MVP and AKN acknowledge support from Russian Science Foundation grant 18-72-00159 for the analysis of the environmental effects for the PANTHEON supernova sample. MVP and AKN acknowledge the Program of Development of M.V. Lomonosov Moscow State University (Leading Scientific School 'Physics of stars, relativistic objects and galaxies'). NP and PR acknowledge the Clermont Auvergne University and the French CNRS-IN2P3 agency for their funding support. We thank the anonymous reviewer for the constructive remarks on the manuscript.

This research has made use of the SIMBAD data base, operated at CDS, Strasbourg, France. We acknowledge the usage of the HyperLeda data base (http://leda.univ-lyon1.fr). This research has made use of the NASA/IPAC Extragalactic Data base (NED), which is funded by the National Aeronautics and Space Administration and operated by the California Institute of Technology. This research has made use of NASA's Astrophysics Data System Bibliographic Services and following PYTHON software packages: MATPLOTLIB (Hunter 2007), NUMPY (van der Walt, Colbert & Varoquaux 2011), SCIPY (Virtanen et al. 2020), PANDAS (McKinney 2010).

DATA AVAILABILITY

The data underlying this article are available in the article. The light-curve parameters for the PANTHEON supernova sample are taken from https://github.com/dscolnic/Pantheon (Scolnic et al. 2018).

REFERENCES

Abbott T. M. C. et al., 2019, ApJ, 872, L30
Aguado D. S. et al., 2019, ApJS, 240, 23
Aldering G. et al., 2002, in Manhart P. K., Sasian J. M., eds, Proc. SPIE Conf. Ser. Vol. 4832 International Optical Design Conference 2002. SPIE, Bellingham, p. 61
Ashall C., Mazzali P., Sasdelli M., Prentice S. J., 2016, MNRAS, 460, 3529
Baade W., 1938, ApJ, 88, 285
Barkhudaryan L. V., Hakobyan A. A., Karapetyan A. G., Mamon G. A., Kunth D., Adibekyan V., Turatto M., 2019, MNRAS, 490, 718
Betoule M. et al., 2014, A&A, 568, A22
Bogomazov A. I., Tutukov A. V., 2011, Astron. Rep., 55, 497
Brout D., Scolnic D., 2020, preprint (arXiv:2004.10206)
Childress M. et al., 2013a, ApJ, 770, 107
Childress M. et al., 2013b, ApJ, 770, 108
Conley A. et al., 2011, ApJS, 192, 1
de Vaucouleurs G., 1959, Handbuch Phys., 53, 275
Domínguez Sánchez H., Huertas-Company M., Bernardi M., Tuccillo D., Fischer J. L., 2018, MNRAS, 476, 3661
Duarte Puertas S., Vilchez J. M., Iglesias-Páramo J., Kehrig C., Pérez-Montero E., Rosales-Ortega F. F., 2017, A&A, 599, A71
Fink M., Kromer M., Hillebrandt W., Röpke F. K., Pakmor R., Seitenzahl I. R., Sim S. A., 2018, A&A, 618, A124
Frieman J. A. et al., 2008, AJ, 135, 338
Galbany L. et al., 2012, ApJ, 755, 125
Graur O. et al., 2014, ApJ, 783, 28
Guy J. et al., 2007, A&A, 466, 11
Guy J. et al., 2010, A&A, 523, A7
Hakobyan A. A., Adibekyan V. Z., Aramyan L. S., Petrosian A. R., Gomes J. M., Mamon G. A., Kunth D., Turatto M., 2012, A&A, 544, A81
Hamuy M., Phillips M. M., Maza J., Suntzeff N. B., Schommer R. A., Aviles R., 1995, AJ, 109, 1
Hamuy M., Phillips M. M., Suntzeff N. B., Schommer R. A., Maza J., Aviles R., 1996a, AJ, 112, 2391
Hamuy M., Phillips M. M., Suntzeff N. B., Schommer R. A., Maza J., Aviles R., 1996b, AJ, 112, 2398
Hamuy M., Trager S. C., Pinto P. A., Phillips M. M., Schommer R. A., Ivanov V., Suntzeff N. B., 2000, AJ, 120, 1479
Helou G., Madore B., 1988, in European Southern Observatory Conference and Workshop Proceedings, No. 29, p. 335
Henne V. et al., 2017, New Astron., 51, 43
Hill R. et al., 2018, MNRAS, 481, 2766
Hoyle F., Fowler W. A., 1960, ApJ, 132, 565
Hsiao E. Y. et al., 2020, ApJ, 900, 140
Hubble E. P., 1926, ApJ, 64, 321
Hubble E. P., 1936, Realm of the Nebulae, Yale University Press, New Haven
Hunter J. D., 2007, Comput. Sci. Eng., 9, 90
Iben I., Jr, Tutukov A. V., 1984, ApJS, 54, 335
Johansson J. et al., 2013, MNRAS, 435, 1680
Jones D. O., Riess A. G., Scolnic D. M., 2015, ApJ, 812, 31
Kasen D., Röpke F. K., Woosley S. E., 2009, Nature, 460, 869
Kessler R. et al., 2009, ApJS, 185, 32
Kim Y.-L., Smith M., Sullivan M., Lee Y.-W., 2018, ApJ, 854, 24
Kim Y.-L., Kang Y., Lee Y.-W., 2019, J. Korean Astron. Soc., 52, 181
Lampeitl H. et al., 2010, ApJ, 722, 566
Léget P. F. et al., 2020, A&A, 636, A46
Lipunov V. M., Panchenko I. E., Pruzhinskaya M. V., 2011, New Astron., 16, 250
LSST Science Collaboration, 2009, preprint (arXiv:0912.0201)
Makarov D., Prugniel P., Terekhova N., Courtois H., Vauglin I., 2014, A&A, 570, A13
Mazzarella J. M., NED Team, 2007, in Shaw R. A., Hill F., Bell D. J., eds, Astronomical Data Analysis Software and Systems XVI ASP Conference Series, Vol. 376. p. 153
McKinney W., 2010, in van der Walt S., Millman J., eds, Proc. 9th Python in Science Conference, Vol. 445. p. 56
Meyers J. et al., 2012, ApJ, 750, 1
Minkowski R., 1941, PASP, 53, 224
Moreno-Raya M. E., Mollá M., López-Sánchez Á. R., Galbany L., Vílchez J. M., Carnero Rosell A., Domínguez I., 2016, ApJ, 818, L19
Neill J. D. et al., 2009, ApJ, 707, 1449
Perlmutter S. et al., 1999, ApJ, 517, 565
Phillips M. M., 1993, ApJ, 413, L105
Polin A., Nugent P., Kasen D., 2019, ApJ, 873, 84
Pruzhinskaya M. V., Gorbovskoy E. S., Lipunov V. M., 2011, Astron. Lett., 37, 663
Pskovskii I. P., 1977, Sov. Astron., 21, 675
Pskovskii Y. P., 1984, Sov. Astron., 28, 658
Rest A. et al., 2014, ApJ, 795, 44
Riess A. G. et al., 1998, AJ, 116, 1009
Riess A. G. et al., 1999, AJ, 117, 707
Riess A. G. et al., 2004, ApJ, 607, 665
Riess A. G. et al., 2007, ApJ, 659, 98
Riess A. G. et al., 2018, ApJ, 853, 126
Rigault M. et al., 2013, A&A, 560, A66
Rigault M. et al., 2015, ApJ, 802, 20
Rigault M. et al., 2018, preprint (arXiv:1806.03849)
Rodney S. A. et al., 2014, AJ, 148, 13
Roman M. et al., 2018, Astron. Astrophys., 615, A68
Rust B. W., 1974, PhD thesis. Oak Ridge National Lab., TN
Ruxton G. D., 2006, Behav. Ecol., 17, 688
Saunders C. et al., 2018, ApJ, 869, 167
Scolnic D. et al., 2014, ApJ, 795, 45
Scolnic D. M. et al., 2018, ApJ, 859, 101
Shen K. J., Toonen S., Graur O., 2017, ApJ, 851, L50
Smith M. et al., 2012, ApJ, 755, 61
Sullivan M. et al., 2003, MNRAS, 340, 1057
Sullivan M. et al., 2006, ApJ, 648, 868
Sullivan M. et al., 2010, MNRAS, 406, 782
Suzuki N. et al., 2012, ApJ, 746, 85
Timmes F. X., Brown E. F., Truran J. W., 2003, ApJ, 590, L83
Tripp R., 1998, A&A, 331, 815
Tully R. B. et al., 2013, AJ, 146, 86
Tully R. B., Courtois H. M., Sorce J. G., 2016, AJ, 152, 50
Umeda H., Nomoto K., Yamaoka H., Wanajo S., 1999, ApJ, 513, 861
van der Walt S., Colbert S. C., Varoquaux G., 2011, Comput. Sci. Eng., 13, 22
Virtanen P. et al., 2020, Nat. Meth., 17, 261
Webbink R. F., 1984, ApJ, 277, 355
Welch B. L., 1947, Biometrika, 34, 28
Wenger M. et al., 2000, A&AS, 143, 9
Whelan J., Iben I., Jr, 1973, ApJ, 186, 1007
Xavier H. S. et al., 2013, MNRAS, 434, 1443
Zheng C. et al., 2008, AJ, 135, 1766

APPENDIX A: SUPPLEMENTARY DATA

Table A1. Host galaxy morphology of Type Ia Supernovae from the PANTHEON sample (Scolnic et al. 2018) found in SIMBAD ([I], Wenger et al. 2000), HyperLEDA ([II], Makarov et al. 2014), NED ([III], Helou & Madore 1988; Mazzarella & NED Team 2007) data bases or individual publications cited in the column 'Reference'. The final type is summarized in column 'Type'. Object ID denotes the supernova survey included in PANTHEON: 0 – low-z, 1 – PS1, 2 – SDSS, 3 – SNLS, 4 – *HST* supernovae.

SN	ID	z_{CMB}	Host galaxy	[I]	[II]	[III]	Type	Reference
2009an	0	0.00931	NGC 4332	Sa	Sa	Sa	Sa	–
2002cr	0	0.01025	NGC 5468	Sc	Sc	Scd	Sc	–
2006bh	0	0.01042	NGC 7329	Sc:	Sbc	Sb	Sbc	–
2002dp	0	0.01045	NGC 7678	Sbc	Sc	Sc	Sc	–
2010Y	0	0.01123	NGC 3392	E	E	E?	E	–
1998dk	0	0.01202	UGC 139	Scd	Sc	Sc?	Sc	–
2002ha	0	0.01224	NGC 6962	Sab	Sa	Sab	Sab	–
2009kk	0	0.01243	2MASX J03494330–0315348	–	–	–	S0	Tully, Courtois & Sorce (2016)
2009kq	0	0.01247	MCG+05-21-01	Sbc	Sc	–	Sc	–
1997E	0	0.01313	NGC 2258	S0	S0	S0	S0	–
1999dq	0	0.01334	NGC 976	Sc	Sbc	Sc:	Sc	–
2008hv	0	0.01359	NGC 2765	S0	S0	S0	S0	–
2005kc	0	0.01390	NGC 7311	Sa	Sab	Sab	Sab	–
2006N	0	0.01408	MCG+11-08-012	–	E	–	E	–
2001fe	0	0.01449	UGC 5129	Sa	Sa	Sa	Sa	–
2004eo	0	0.01457	NGC 6928	Sab	Sab	Sab	Sab	–
2004ey	0	0.01462	UGC 11816	Sbc	SBc	Sc:	Sbc	–
2005el	0	0.01489	NGC 1819	S0	S0	S0	S0	–
2006hb	0	0.01496	MCG-04-12-034	E/S0	E-S0	E?	E/S0	–
2006td	0	0.01504	2MASX J01581578+3620538	S	Sc	–	Sc	–
2007ca	0	0.01515	MCG-02-34-61	Sc	Sc	Sc	Sc	–
2009nq	0	0.01526	NGC 7549	Sbc	Sc	Scd	Sc	–
1999ej	0	0.01544	NGC 495	S0a	S0-a	S0/a	S0/a	–
2001en	0	0.01544	NGC 523	Sb	Sbc	–	Sbc	–
2005bo	0	0.01556	NGC 4708	Sab	Sa	Sab	Sab	–
2007A	0	0.01595	NGC 105	Sbc	Sab	–	Sbc	–
2001V	0	0.01596	NGC 3987	Sb	Sb	Sb	Sb	–
2000dk	0	0.01602	NGC 382	E:	E	E:	E	–
1998ef	0	0.01602	UGC 646	S	Sb	S?	Sb	–
1994S	0	0.01611	NGC 4495	E	Sab	Sab	Sab	–
2010H	0	0.01621	IC 494	S0	S0	S0:	S0	–
2001da	0	0.01647	NGC 7780	Sab	Sa	Sab	Sab	–
2007ap	0	0.01668	MCG+03-41-003	S0	S0-a	S0	S0/a	–
1996bv	0	0.01673	UGC 3432	Sc	Sc	Scd:	Sc	–
1997Y	0	0.01678	NGC 4675	Sb	Sb	Sb:	Sb	–
2007fb	0	0.01681	UGC 12859	Sbc	Sbc	Sbc	Sbc	–
2006ef	0	0.01682	NGC 809	S0	S0	S0:	S0	–
1993ae	0	0.01693	UGC 1071	E		S?	E	–
2009le	0	0.01703	2MASX J02091807–2324542	Sc	Sbc	Sbc	Sbc	–
2001G	0	0.01707	MCG+08-17-043		Sab	Sc	Sab	–
2008C	0	0.01708	UGC 3611	S0a	S0-a	S0/a	S0/a	–
2008L	0	0.01730	NGC 1259	E	E-S0	–	E	–
2006ax	0	0.01773	NGC 3663	Sb	Sbc	Sbc	Sbc	–
2006ej	0	0.01916	IC 1563	S0	S0	S0	S0	–
2002kf	0	0.01948	2MASX J06371661+4951005	–	–	–	Sc	Tully et al. (2016)
2010A	0	0.01985	UGC 2019	I...	Sbc	S?	Sbc	–
2008ds	0	0.01994	UGC 299	Sc	Sc	Sc	Sc	–
1998ec	0	0.02010	UGC 3576	Sb	Sb	Sb	Sb	–
2000B	0	0.02045	NGC 2320	E	E	E	E	–
2009ds	0	0.02050	NGC 3905	Sc	Sc	Sc	Sc	–
2005ki	0	0.02066	NGC 3332	E	E-S0	S0	E	–
2006bq	0	0.02146	NGC 6685	E/S0	E-S0	S0:	E/S0	–
2006et	0	0.02160	NGC 232	Sa	Sa	Sa?	Sa	–
2006or	0	0.02167	NGC 3891	Sc	Sbc	Sbc	Sbc	–
2000fa	0	0.02180	UGC 3770	I	I	Im	Ir	–
2007bc	0	0.02187	UGC 6332	Sab	Sa	Sa	Sa	–
1995ak	0	0.02193	IC 1844	Sbc	Sbc	–	Sbc	–
2009na	0	0.02212	UGC 5884	Sc	Sb	Sb:	Sb	–
2006mp	0	0.02280	MCG+08-31-029	–	–	–	Sb	Tully et al. (2016)
2006sr	0	0.02298	UGC 14	Sc	Sc	S?	Sc	–
2000cn	0	0.02321	UGC 11064	Sc	Sc	Scd:	Sc	–
2006cp	0	0.02334	UGC 7357	Sd	Sc	Sc	Sc	–

Table A1 – *continued*

SN	ID	z_{CMB}	Host galaxy	[I]	[II]	[III]	Type	Reference
1998eg	0	0.02362	MCG+01-57-014	Sc	Sc	Scd:	Sc	–
2006ac	0	0.02395	NGC 4619	Sc	Sb	Sb	Sb	–
2003it	0	0.02419	UGC 40	S	Sb	S?	Sb	–
2007F	0	0.02419	UGC 8162	Scd	Sc	Scd:	Scd	–
1994M	0	0.02431	NGC 4493	S0	E	E	E	–
2008bf	0	0.02453	NGC 4055	E:	E	E:	E	–
2009D	0	0.02466	MCG-03-10-52	Sb	Sb	Sb	Sb	–
2002bf	0	0.02474	2MASX J10154226+5540030	Sbc	Sb	Sb:	Sb	–
2002he	0	0.02484	UGC 4322	E	E	E	E	–
2007cq	0	0.02510	2MASX J22144070+0504435	–	–	–	Sbc	Hakobyan et al. (2012)
2006bb	0	0.02524	UGC 4468	S0	S0	S0	S0	–
2005M	0	0.02562	NGC 2930	–	Sbc	S?	Sbc	–
1999X	0	0.02577	2MASX J08543185+3630346		Sa	Sa	Sa	–
2005ms	0	0.02590	UGC 4614	Sd	Sb	S?	Scd	Hakobyan et al. (2012)
2005mc	0	0.02602	UGC 4414		S0-a	S0/a	S0/a	–
370356	1	0.02640	UGC 7228	Sab	Sb	–	Sb	–
2007co	0	0.02656	MCG+05-43-016	–	–	–	Sc	Tully et al. (2016)
2007su	0	0.02662	LEDA 3374128	–	–	–	SF	Hakobyan et al. (2012)
2001gb	0	0.02676	IC 582	Sd	Sb	S	Sc	Hakobyan et al. (2012)
2005na	0	0.02683	UGC 3634	Sa	Sa	Sa	Sa	–
2008ar	0	0.02739	IC 3284	Sa	Sab	Sab	Sab	–
1996C*	0	0.02752	MCG+08-25-047	Sa	Sb	–	Sb	–
2006ev	0	0.02762	UGC 11758	S	Sbc	S?	Sbc	–
2005eq	0	0.02788	MCG-01-09-006	Sbc	S?	Scd?	Sbc	–
2003U	0	0.02818	UGC 10832	Sc	Sc	Scd:	Sc	–
2002de	0	0.02827	NGC 6104	S0	Sb	S?	Sb	–
2009ad	0	0.02834	UGC 3236	Sbc	Sb	Sbc	Sbc	–
2006qo	0	0.02885	UGC 4133	Sc	Sc	Scd:	Sc	–
2003ch	0	0.02922	UGC 3787	E/S0	E-S0	S0?	E/S0	–
1994Q	0	0.02956	2MASX J16495110+4025599	S/Irr	Sc	Scd	Sc	–
2007is	0	0.02968	UGC 10553	S/Irr	Sab	Sab:	Sab	–
2004ef	0	0.02979	UGC 12158	Sb	Sb	Sb	Sb	–
2007cc	0	0.03002	2MASX J14084200–2135498	S...	Sc	Sc	Sc	–
2002ck	0	0.03031	UGC 10030	Sb	Sab	Sb	Sab	–
2007ux	0	0.03043	2MASX J10091969+1459268	–	S0-a		S0/a	–
PTF10bjs	0	0.03052	MCG+09-21-083	–	Sb	Sb	Sb	–
2006bw	0	0.03079	LEDA 1258718	–	E	–	E	–
2006en	0	0.03080	MCG+05-54-41	Sc	Sc	–	Sc	–
1999cc	0	0.03153	NGC 6038	Sbc	Sc	Sc	Sc	–
2005lu	0	0.03154	MCG-03-07-40	Sd	Sbc	S.../Irr?	Sbc	–
10026	1	0.03160	MCG+10-15-120	Sd	Sc	–	Sc	–
2007bd	0	0.03185	UGC 4455	Sab	Sa	Sa	Sa	–
2006te	0	0.03210	2MASX J08114347+4133184	Sbc	S?	–	Sbc	–
2004as	0	0.03213	LEDA 1676859	S/I	Sd	–	Sd	–
2007ob	0	0.03266	2MASX J23122598+1354503	S0	S0-a	S0	S0	–
2008bw	0	0.03276	UGC 11241	Sb	Sb	Sb	Sb	–
1997dg	0	0.03280	LEDA 5065169	–	–	–	Scd	Hakobyan et al. (2012)
2008gp	0	0.03285	MCG+00-09-074	Sb	Sa	Sa	Sa	–
2005iq	0	0.03295	MCG-03-01-08	Sa	Sab	Sa	Sa	–
2008gl	0	0.03297	UGC 881	E	E	E	E	–
2004L	0	0.03341	MCG+03-27-38	Sb	Sc	–	Sc	–
2006gr	0	0.03344	UGC 12071	Sb	Sb	Sb	Sb	–
2003iv	0	0.03358	MCG+02-08-14	E...	E	–	E	–
2008bq	0	0.03360	2MASX J06410310–3802083	Sa	Sab	Sa	Sa	–
2003cq	0	0.03375	NGC 3978	S	Sb	Sbc:	Sb	–
2003ae	0	0.03380	2MASX J09282257+2726402	–	S?	–	Sbc	Tully et al. (2013)
2008af	0	0.03411	UGC 9640	E	E	E	E	–
2005be	0	0.03416	2MASX J14593310+1640070	Sa	S0-a	–	S0/a	–
2002G	0	0.03449	MCG+06-29-043	Sa	E-S0	–	Sa	–
1996bl	0	0.03481	2MASX J00361813+1123354	–	–	–	Sbc	Hakobyan et al. (2012)
2008at	0	0.03513	UGC 5645	Sb	Sb	Sb	Sb	–
2007hu	0	0.03540	NGC 6261	Sa	S0-a	S0/a	S0/a	–
2006mo	0	0.03597	MCG+06-02-17	S...	Sc	S?	Sc	–
2008gb	0	0.03640	UGC 2427	Sbc	Sbc	Sb-c	Sbc	–
2000cf	0	0.03646	MCG+11-19-25	–	Sbc	–	Sbc	–

Table A1 – *continued*

SN	ID	z_{CMB}	Host galaxy	[I]	[II]	[III]	Type	Reference
17784	2	0.03652	SDSS J032950.83+000316.0	–	Sc	–	Sc	–
2007O	0	0.03659	UGC 9612	Sbc	Sc	Sc	Sc	–
2002eu	0	0.03671	2MASX J01494273+3237303	S0/Sa	–	–	S0/a	–
2006je	0	0.03712	2MASX J01505173+3305321	Sa	S0	–	S0	–
2007cb	0	0.03753	2MASX J13581715–2322179	Sab	Sb	Sa-b	Sab	–
2002bz	0	0.03762	MCG+05-34-033	dG	E	S?	S0	–
1999ef	0	0.03799	UGC 607	Sc	Sc	Scd?	Sc	–
2006ak	0	0.03890	2MASX J11093314+2837393	–	S0	–	Sab	Tully et al. (2016)
2008051	0	0.03908	SDSS J151958.87+045416.8	–	–	–	SF	Jones et al. (2015)
2005lz	0	0.03917	UGC 1666	–	–	–	Sa	Tully et al. (2016)
2003fa	0	0.04016	MCG+07-36-033	Sb:...	Sb	S?	Sb	–
2001az	0	0.04059	UGC 10483	S	Sbc	S	Sbc	–
2007kk	0	0.04119	UGC 2828	Sb	Sb	Sbc	Sb	–
2005hf	0	0.04205	2MASX J01270614+1906587	–	–	–	Sa	Hakobyan et al. (2012)
2007nq	0	0.04243	UGC 595	E	E	S?	E	–
2001ic	0	0.04296	NGC 7503	E...	E	E:	E	–
2006gt	0	0.04362	2MASX J00561810–0137327	–	–	–	Sc	Tully et al. (2013)
10805	2	0.04397	2MASX J22594265–0000478	Sm/Im	E?	–	Ir	–
2005hc	0	0.04497	MCG+00-06-03	E/S0	Sbc		Sab	Tully et al. (2016)
2008by	0	0.04584	SDSSJ120520.81+405644.4	–	–	–	SF	Jones et al. (2015)
360156	1	0.04620	SDSS J100313.51+015343.2	S	Sc	–	Sc	–
2004gu	0	0.04698	2MASX J12462478+1156577	–	S?	–	Sab	Tully et al. (2016)
2008050	0	0.04702	ULAS J133647.52+050829.6	–	–	–	SF	Childress et al. (2013a)
2006eq	0	0.04834	2MASX J21283758+0113490	–	E?	–	Sbc	Tully et al. (2013)
2006cq	0	0.04921	IC 4239	S...	S0-a	S?	S0/a	–
530086	1	0.05020	LEDA 1153699	–	E-S0	–	E/S0	–
1993ac	0	0.05021	LEDA 17787	E	E	–	E	–
2006ah	0	0.05097	LEDA 994819	–	–	–	SF	Childress et al. (2013a)
2010dt	0	0.05294	2MASX J16431345+3240391	–	Sb	Sb	Sb	–
2007ar	0	0.05335	MCG+10-19-62	S0	E-S0	E	S0	–
2008ac	0	0.05351	LEDA 2317123	–	S?	–	Sc	Hakobyan et al. (2012)
1998dx	0	0.05389	UGC 11149	Es...	–	–	E	–
490007	1	0.05470	SDSS J121704.45+463737.0	–	S?	–	SF	Aguado et al. (2019)
19968	2	0.05490	2MASX J01372378–0018422	–	E	–	E	–
2003ic	0	0.05491	MCG-02-02-086	E	S0	S0	E	–
2005hj	0	0.05592	LEDA 4131950	–	–	–	SF	Hakobyan et al. (2012)
2006py	0	0.05661	LEDA 3333560	–	E	–	E	–
2006ob	0	0.05824	UGC 1333	Sa	Sb	Sb:	Sb	–
2006oa	0	0.05884	LEDA 4019108	–	–	–	SF	Hakobyan et al. (2012)
2001ah	0	0.05891	UGC 6211	Sc	Sbc	Sbc	Sbc	–
2008bz	0	0.06143	2MASX J12385810+1107502	–	Sc	–	Sc	–
2007ae	0	0.06416	UGC 10704	S	Sbc	S	Sbc	–
10028	2	0.06426	2MASX J01105805+0016343	E/S0	E	–	E/S0	–
6057	2	0.06651	LEDA 1130011	Sm/Im	S?	–	Sb	Hakobyan et al. (2012)
2006cj	0	0.06839	2MASX J12592407+2820498	–	S?	–	Sb	Hakobyan et al. (2012)
2006on	0	0.06884	LEDA 4524675	–	E?	–	E	–
2006al	0	0.06905	LEDA 3358371	–	E?	–	S0/a	Tully et al. (2016)
2008Y	0	0.07029	MCG+09-19-039	–	Sbc	–	Sbc	–
17240	2	0.07153	SDSS J003434.00–011257.5	–	E	–	E	–
2003hu	0	0.07472	2MASX J19113272+7753382	–	–	–	Sbc	Hakobyan et al. (2012)
7876	2	0.07489	LEDA 3116670	Sb	E?	–	Sb	–
17186	2	0.07849	Anon J020627–0053	–	–	–	SF	Hakobyan et al. (2012)
12779	2	0.07891	LEDA 1188169	S	Sbc		Sbc	–
12950	2	0.08141	SDSS J232640.14–005026.2	–	E?	–	SF	Hakobyan et al. (2012)
130308	1	0.08220	LEDA 2422566	–	S?	–	SF	Duarte Puertas et al. (2017)
12781	2	0.08282	2MASX J00213789–0100383	–	E-S0	–	E/S0	–
722	2	0.08504	2MASS J00024907+0045051	E/S0	E	–	E	–
3592	2	0.08543	2MASX J01161269+0047265	Sb	Sa	–	Sb	–
21502	2	0.08784	2MASX J23342408–0053250	–	E	–	E	–
1241	2	0.08848	SDSS J223041.15–004634.5	–	–	–	Pa	Jones et al. (2015)
590194	1	0.08960	SDSS J084056.87+443127.3	–	–	–	SF	Aguado et al. (2019)
774	2	0.09227	SDSS J014151.28–005236.2	Sa	S?	–	Pa	Jones et al. (2015)
18241	2	0.09391	SDSS J204933.00–004543.0	–	–	–	SF	Jones et al. (2015)
2102	2	0.09401	SDSS J204853.04+001129.8	Sm/Im	–	–	Ir	–
420100	1	0.09630	SDSS J221225.28+005104.8	S0	E	–	E	–

Table A1 – *continued*

SN	ID	z_{CMB}	Host galaxy	[I]	[II]	[III]	Type	Reference
10010	1	0.09940	SDSS J100325.83+010143.3	–	–	–	SF	Jones et al. (2015)
10434	2	0.10288	2MFGC 16592	E/S0	Sc	–	E/S0	–
13135	2	0.10337	SDSS J001641.85–002530.5	–	E-S0	–	E/S0	–
20064	2	0.10351	2MASX J23542073–0055023	–	Sa	–	Sa	–
18697	2	0.10638	SDSS J004453.81–005948.6	–	–	–	SF	Hakobyan et al. (2012)
20625	2	0.10683	SDSS J002243.95–002845.8	–	E	–	SF	Hakobyan et al. (2012)
500038	1	0.10720	COSMOS 2334037	–	–	–	SF	Aguado et al. (2019)
21034	2	0.10750	SDSS J015234.16+011438.8	–	Sb		Sbc	Hakobyan et al. (2012)
7147	2	0.10886	SDSS J232004.44–000320.1	E/S0	–	–	E/S0	–
20027	1	0.10980	SDSS J122520.40+460059.2	–	Sbc	–	Sbc	–
18612	2	0.11364	SDSS J004909.12+003547.8	–	S0-a	–	S0/a	–
8719	2	0.11628	SDSS J003053.26–004307.0	Sm/Im	–	–	Ir	–
5395	2	0.11635	SDSS J031833.80+000724.0	Sbc/Sc	–	–	Sc	–
2561	2	0.11741	2MASX J03052260+0051346	Sb	E	–	Sb	–
16259	2	0.11771	LEDA 1177432	–	E	–	E	–
1371	2	0.11797	SDSS J231729.69+002546.8	E/S0	E?	–	E/S0	–
19953	2	0.12190	SDSS J221143.27+003445.5	–	–	–	SF	Aguado et al. (2019)
18835	2	0.12262	SDSS J033444.49+002119.8	–	–	–	Pa	Hakobyan et al. (2012)
2916	2	0.12303	Anon J220341+0034	–	–	–	Sa	Zheng et al. (2008)
16021	2	0.12336	SDSS J005522.52–002321.1	–	–	–	SF	Aguado et al. (2019)
6406	2	0.12376	SDSS J030421.25–010347.1	Sb	–	–	Sb	–
13044	2	0.12455	SDSS J221010.32+003014.1	Sc	–	–	Sc	–
2992	2	0.12608	SDSS J034159.34–004658.4	Sb	–	–	Sab	Zheng et al. (2008)
16069	2	0.12688	SDSS J224458.81–010022.9	–	–	–	SF	Hakobyan et al. (2012)
744	2	0.12694	SDSS J215647.64+001901.3	Sm/Im	–	–	SF	Aguado et al. (2019)
18855	2	0.12715	SDSS J031432.11+001608.0	–	–	–	SF	Hakobyan et al. (2012)
18809	2	0.12837	SDSS J032331.35+004002.1	–	–	–	Pa	Hakobyan et al. (2012)
22075	2	0.12899	SDSS J015951.28+011259.7	–	–	–	Pa	Hakobyan et al. (2012)
1032	2	0.12903	SDSS J030711.01+010711.9	Sa	–	–	Sa	–
5751	2	0.12928	SDSS J004632.24+005017.3	Sbc/Sc	–	–	Sbc	–
17280	2	0.13045	SDSS J034310.04+000614.2	–	–	–	Sbc	Hakobyan et al. (2012)
15508	2	0.13353	SDSS J014840.67–003432.7	–	–	–	SF	Aguado et al. (2019)
15234	2	0.13514	SDSS J010749.93+004942.9	–	–	–	SF	Hakobyan et al. (2012)
17629	2	0.13639	SDSS J020232.75–010523.7	S	–	–	SF	Aguado et al. (2019)
18602	2	0.13696	SDSS J223556.07+003632.7	–	–	–	SF	Aguado et al. (2019)
21062	2	0.13729	SDSS J221343.61+002346.6	–	–	–	SF	Aguado et al. (2019)
17366	2	0.13811	SDSS J210308.39–010152.2	–	–	–	SF	Hakobyan et al. (2012)
190340	1	0.13840	SDSS J221632.39+002824.3	–	–	–	SF	Aguado et al. (2019)
1794	2	0.14070	SDSS J211120.86–002643.4	Sm/Im	–	–	Ir	–
2635	2	0.14310	SDSS J033048.96–011415.4	Sbc/Sc	–	–	Sc	–
17497	2	0.14387	SDSS J022832.76–010234.1	–	–	–	SF	Hakobyan et al. (2012)
8921	2	0.14409	SDSS J214000.47–000029.0	Sm/Im	–	–	Ir	–
17605	2	0.14533	SDSS J203648.61+000554.6	–	–	–	SF	Aguado et al. (2019)
2031	2	0.15186	SDSS J204810.43–011016.8	Sm/Im	–	–	Ir	–
19353	2	0.15325	SDSS J025227.18+001506.2	–	–	–	SF	Hakobyan et al. (2012)
5550	2	0.15492	SDSS J001423.63+001959.4	–	–	–	Sb	–
18030	2	0.15517	SDSS J001943.97–002400.4	–	–	–	SF	Hakobyan et al. (2012)
13354	2	0.15653	SDSS J015015.53–005312.1	–	–	–	SF	Hakobyan et al. (2012)
17171	2	0.15899	SDSS J214600.83–011309.6	–	–	–	Pa	Hakobyan et al. (2012)
3317	2	0.15990	SDSS J014751.04+003825.5	Sm/Im	–	–	Ir	–
2689	2	0.16035	SDSS J013936.00–004528.5	–	–	–	Pa	Hakobyan et al. (2012)
3087	2	0.16431	SDSS J012137.58–005837.7	Sm/Im	–	–	Ir	–
19616	2	0.16455	SDSS J022823.91+001109.6	–	–	–	SF	Hakobyan et al. (2012)
20764	2	0.16477	SDSS J014428.99+001347.2	–	–	–	SF	Aguado et al. (2019)
12843	2	0.16595	SDSS J213530.83–005846.6	–	–	–	Pa	Hakobyan et al. (2012)
12856	2	0.17028	SDSS J221127.68+004520.1	–	–	–	SF	Hakobyan et al. (2012)
3080	2	0.17315	SDSS J010743.60–010222.1	Sa		–	Sa	–
15648	2	0.17383	SDSS J205452.51–001144.9	–		–	Pa	Hakobyan et al. (2012)
14421	2	0.17400	SDSS J020719.18+011507.2	–	–	–	Pa	Hakobyan et al. (2012)
19969	2	0.17428	SDSS J020738.36–001926.5	–	–	–	SF	Hakobyan et al. (2012)
5635	2	0.17839	SDSS J221243.88–000206.2	Sm/Im	–	–	Ir	–
6936	2	0.17890	SDSS J213256.13–004200.2	Sm/Im	–	–	Ir	–
2372	2	0.17958	SDSS J024205.00–003227.7	E/S0	–	–	E/S0	–
13254	2	0.17990	SDSS J024814.09–002048.5	–	–	–	SF	Hakobyan et al. (2012)
14284	2	0.18037	SDSS J031611.84–003603.5	–	–	–	Pa	Hakobyan et al. (2012)

Table A1 – *continued*

SN	ID	z_{CMB}	Host galaxy	[I]	[II]	[III]	Type	Reference
17215	2	0.18079	LEDA 1184310	–	–	–	Sab	Hakobyan et al. (2012)
15443	2	0.18123	SDSS J031928.18–001904.8	–	–	–	SF	Hakobyan et al. (2012)
15421	2	0.18443	SDSS J021457.91+003609.7	–	–	–	SF	Hakobyan et al. (2012)
8213	2	0.18468	SDSS J235005.06–005517.5	Sbc/Sc	–	–	Sbc	–
6304	2	0.18979	SDSS J014559.74+011144.4	Sm/Im	–	–	Ir	–
762	2	0.19009	SDSS J010208.65–005246.7	Sa	–	–	Sa	–
2246	2	0.19422	SDSS J032021.71–005305.3	Sm/Im	–	–	Ir	–
16099	2	0.19580	SDSS J014541.09–010316.5	–	–	–	SF	Hakobyan et al. (2012)
15129	2	0.19611	SDSS J211536.49–001918.1	–	–	–	SF	Hakobyan et al. (2012)
13070	2	0.19718	SDSS J235108.37–004447.6	–	–	–	SF	Hakobyan et al. (2012)
15222	2	0.19801	SDSS J001124.57+004207.2	–	–	–	E/S0	Hakobyan et al. (2012)
7243	2	0.20323	SDSS J215219.02+002818.9	Sm/Im		–	Ir	–
17801	2	0.20515	SDSS J210422.51–005354.4	–	–	–	Sb	Hakobyan et al. (2012)
19913	2	0.20557	SDSS J221502.93–002030.1	S0/a	–	–	S0/a	–
7847	2	0.21160	SDSS J020950.32–000342.1	Sb	–	–	Sb	–
2330	2	0.21179	SDSS J002713.76+010715.0	Sb	–	–	Sb	–
8495	2	0.21353	SDSS J222102.64–004454.2	Sb	–	–	Sb	–
9467	2	0.21885	SDSS J215548.23+011052.6	Sa	–	–	Sa	–
5533	2	0.21887	SDSS J215440.79+002446.0	Sm/Im	–	–	Ir	–
13072	2	0.22916	SDSS J221950.56+000125.2	–	–	–	SF	Hakobyan et al. (2012)
3452	2	0.22967	SDSS J221841.11+003822.2	Sm/Im	–	–	Ir	–
12971	2	0.23380	SDSS J002635.42–001811.8	–	–	–	Pa	Hakobyan et al. (2012)
13511	2	0.23652	SDSS J024226.71–004739.2	–	–	–	Pa	Xavier et al. (2013)
3377	2	0.24448	SDSS J033637.48+010443.7	Sm/Im	–	–	Ir	–
3451	2	0.24835	SDSS J221616.45+004228.1	Sa	–	–	Sa	–
15161	2	0.24852	SDSS J022322.22+004908.4	–	–	–	SF	Hakobyan et al. (2012)
3199	2	0.24961	SDSS J221309.91+010301.6	Sb	–	–	Sb	–
5717	2	0.25037	SDSS J011135.04–000021.4	Sm/Im	–	–	Ir	–
9032	2	0.25249	SDSS J223132.24–002937.1	Sm/Im	–	–	Ir	–
1112	2	0.25609	SDSS J223604.05–002229.7	Sb	–	–	Sb	–
9457	2	0.25672	SDSS J222315.51+001513.3	Sa	–	–	Sa	–
8046	2	0.25760	SDSS J023628.25+003042.6	E/S0	–	–	E/S0	–
6108	2	0.25800	SDSS J000713.57+002056.7	Sm/Im	–	–	Ir	–
2017	2	0.26162	SDSS J215546.53+003536.4	Sbc/Sc	–	–	Sbc	–
1253	2	0.26166	SDSS J213511.66+000946.2	Sbc/Sc	–	–	Sbc	–
2943	2	0.26405	Anon J011049+0100	Sm/Im	–	–	Ir	–
13099	2	0.26451	SDSS J235916.47–011502.5	–	–	–	SF	Hakobyan et al. (2012)
6315	2	0.26576	SDSS J204155.82+010530.7	Sm/Im	–	–	Ir	–
6192	2	0.27091	SDSS J231351.64+011526.2	Sm/Im	–	–	Ir	–
4000	2	0.27656	SDSS J020404.01–002158.7	Sm/Im	–	–	Ir	–
5957	2	0.27923	SDSS J021902.35–001621.2	Sm/Im	–	–	Ir	–
6196	2	0.27980	SDSS J223031.48–003008.6	E/S0	–	–	E/S0	–
2789	2	0.28890	SDSS J225648.48+002402.0	E/S0	–	–	E/S0	–
6249	2	0.29353	SDSS J001303.75–003712.9	Sm/Im	–	–	Ir	–
13610	2	0.29683	SDSS J214403.41+004331.7	–	–	–	SF	Hakobyan et al. (2012)
6137	2	0.29888	SDSS J203144.52+001441.8	Sbc/Sc	–	–	Sbc	–
5391	2	0.30021	SDSS J032922.16–010542.9	Sm/Im	–	–	Ir	–
6699	2	0.30915	SDSS J213115.63–010326.3	Sb	–	–	Sb	–
5844	2	0.30929	SDSS J215108.58–005034.0	Sm/Im	–	–	Ir	–
16211	2	0.30938	SDSS J231239.09+001557.5	–	–	–	Pa	Hakobyan et al. (2012)
4241	2	0.33051	SDSS J004857.01–005419.8	Sm/Im	–	–	Ir	–
4679	2	0.33103	SDSS J012606.79+004036.9	Sm/Im	–	–	Ir	–
05D3jr	3	0.37039	[HSP2005] J141928.768+525153.34	E	–	–	E	–
7779	2	0.37986	SDSS J204019.15–000022.8	Sbc/Sc	–	–	Sbc	–
18721	2	0.40127	SDSS J001218.66–000439.5	–	–	–	Pa	Hakobyan et al. (2012)
Vilas	4	0.93500	–	–	–	–	Early-type	Meyers et al. (2012)
Patuxent	4	0.97000	–	–	–	–	Late-type	Meyers et al. (2012)
Ombo	4	0.97520	–	–	–	–	Late-type	Meyers et al. (2012)
SCP05D0	4	1.01400	–	–	–		Early-type	Meyers et al. (2012)
Eagle	4	1.02000	–	–	–	–	Late-type	Meyers et al. (2012)
SCP06C0	4	1.09200	–	–	–	–	Early-type	Meyers et al. (2012)
Gabi	4	1.12000	–	–	–	–	Late-type	Meyers et al. (2012)
vespesian†	4	1.20600	–	–	–	–	E/S0	Rodney et al. (2014)
Lancaster	4	1.23000	–	–	–	–	Early-type	Meyers et al. (2012)
Koekemoer	4	1.23000	–	–	–	–	Late-type	Meyers et al. (2012)

Table A1 – *continued*

SN	ID	z_{CMB}	Host galaxy	[I]	[II]	[III]	Type	Reference
Aphrodite	4	1.30000	–	–	–	–	Late-type	Meyers et al. (2012)
Thoth	4	1.30500	–	–	–	–	Early-type	Meyers et al. (2012)
washington	4	1.33000	[RRS2014] GSD11Was Host G	–	–	–	Sb/Sbc/Sc	Rodney et al. (2014)
Mcguire	4	1.37000	–	–	–	–	Late-type	Meyers et al. (2012)
Sasquatch	4	1.39000	–	–	–	–	Early-type	Meyers et al. (2012)
Primo	4	1.55000	–	–	–	–	Scd/Ir	Rodney et al. (2014)
wilson	4	1.91400	–	–	–	–	E/S0	Rodney et al. (2014)
colfax	4	2.26000	–	–	–	–	E/S0	Rodney et al. (2014)

Notes. ⋆The coordinates for SN 1996C given in PANTHEON ($\alpha = 207.751587,\ \delta = +49.341251$) are wrong. The correct coordinates are $\alpha = 207.7025,\ \delta = +49.318639$.
†The coordinates for the Hubble SN Vespesian given in PANTHEON ($\alpha = 215.136078,\ \delta = +53.046726$) in fact correspond to another Hubble SN – Obama. According to Riess et al. (2018) the coordinates of SN Vespasian (CLF11Ves) are $\alpha = 322.4275,\ \delta = -7.696583$.

This paper has been typeset from a TEX/LATEX file prepared by the author.